Kang et al. Fashion and Textiles (2024) 11:1
https://doi.org/10.1186/s40691-023-00356-6

Fashion and Textiles

RESEARCH Open Access

Facile fabrication and characterization of MXene/cellulose composites for electrical properties, electric heating performance

Chan Sol Kang[1], Jong Kyu Kim[2], Chae-Seok Lee[3], HoJong Chang[3*], Yeong Heon Cho[4], Cheera Prasad[5] and Hyeong Yeol Choi[5*]

*Correspondence:
hojoungc@kaist.ac.kr;
spaachoi@dau.ac.kr

[1] Department of Advanced Materials Engineering, Shinhan University, Uijeongbu 11644, Republic of Korea
[2] Department of Energy Engineering, Shinhan University, Uijeongbu 11644, Republic of Korea
[3] KAIST Convergence Research Center for College of Engineering, Daejeon 34141, Republic of Korea
[4] Department of Chemical Engineering, Dong-A University, Busan 49315, Republic of Korea
[5] Department of Fashion Design, Dong-A University, Busan 49315, Republic of Korea

Abstract

Developing energy-efficient and multifunctional wearable electronic textiles (E-textiles) is a significant challenge. This study investigates MXene-coated cellulose hybrid fibers, focusing on their electrical properties, heating performance, and thermal stability. The fabrication process involves continuous dipping of cellulose fibers into an aqueous MXene solution, resulting in the creation of MXene-coated cellulose hybrid fibers. We confirm the uniform coating of MXene sheets on the cellulose fiber surfaces, with increasing content throughout the dip coating cycle, as evidenced by X-ray diffraction and scanning electron microscopy analysis. The high thermal conductivity of MXene acts as a heat source, impacting the thermal stability of cellulose fibers at lower temperatures. Additionally, the electrical properties of MXene/cellulose hybrid fiber composites are influenced at elevated temperatures. Remarkably, the longitudinal electrical conductivity of the MXene-coated cellulose fiber composites exhibits a notable increase of 0.06 S/cm after the final coating cycle, demonstrating the effective and conductive nature of the layer-by-layer MXene network formed on the cellulose fibers.

Keywords: MXenes, Cellulose fiber, Electrical properties, Electro-heating, E-textile

Introduction

The rapid advancement of flexible and wearable electronic devices, capable of comfortable integration with the human body, has been driven by the growing need for improved quality of life. These devices aim to convert diverse environmental and physiological stimuli into measurable electrical signals, such as resistance and capacitance (Trung et al., 2016; Gao et al., 2019; Wang et al., 2009a, 2009b). Flexible electronic materials have shown great promise across numerous applications, including soft robotics, electronic skin, human health monitoring, and human–machine interfaces (Kim et al., 2023; Lee et al., 2020; Lei et al., 2017; Liu et al., 2020; Wang et al., 2020; Wu et al., 2015; Yang et al., 2019; Zhang et al., 2020; Zhong et al., 2019). Consequently, substantial efforts have been dedicated to the development of various flexible electronic materials. Among the possibilities, everyday textiles have gained significant attention due to their lightweight nature, flexibility, biocompatibility, washability, and resemblance to human tissue (Chen et al., 2020; Seyedin et al., 2019; Zhang et al., 2019).

The realization of the aforementioned functions in E-textiles necessitates the integration of conductivity with electrochemically dynamic materials. To this end, extensive research has been conducted on techniques that utilize 2D materials, including metals, carbon nanotubes (CNTs), conductive polymers, and composites such as MXene and graphene oxide, to transform yarn into patterned fabrics and electronic fiber materials (Kim & Lee, 2018, 2020; Yin et al., 2020; Chen et al., 2019). MXenes have emerged as promising functional fillers for fiber materials due to their notable mechanical modulus, high electrical conductivity, thermal stability, and thermal conductivity. These materials are commonly obtained by selectively extracting specific atoms (referred to as A elements) from layered ternary transition metal carbides (known as $M_{n+1}AX_n$ phases). By use of the etching procedure, MXenes typically have the formula $M_{n+1}X_nT_x$, where M is an early transition metal (Ti, V, Mo, etc.), X is a symbol for C or N, n is 1, 2, or 3, and T_x stands for surface terminal groups (O, F and OH) (Alhabeb et al., 2017; Naguib et al., 2014). MXene nanosheets are terminated with surface moieties as a result of the watery medium utilized during the synthesis, and these surface terminations provide MXenes with their hydrophilicity. $Ti_3C_2T_x$ MXenes, two-dimensional transition metal carbides, are thought to be potential alternatives because of their exceptional metal electrical conductivity, high hydrophilicity, and abundant surface functional groups, which are advantageous for good adhesion between the polymer matrix and conductive filler and uniform diffusion (Liang et al., 2019; Zhou et al., 2020). To illustrate the capabilities of MXenes, a notable example involves the uniform coating of MXenes onto the framework of a sponge substrate without prior preparation. This coating process yielded remarkable outcomes, including high sensitivity (442 kPa^{-1}) and an extensive sensing range (0–18.56 kPa). These desirable characteristics were attributed to the exceptional diffusion properties of MXenes and the strong interaction established between the sponge substrate and MXene coating (Yue et al., 2018).

According to some reports, MXene sheets have garnered significant attention for their potential applications in various forms, including macroscopic films and foams, as well as nanofillers in polymer composites (Cui et al., 2019; Wang et al., 2009a, 2009b). Notably, Shahzad et al. successfully created a highly conductive MXene thin film with exceptional electromagnetic interference (EMI) shielding properties (Shahzad et al., 2016). Liu et al. developed a foaming method to produce flexible, hydrophobic, and lightweight MXene foams, that exhibited outstanding EMI-shielding performance and water resistance (Liu et al., 2017). In addition, researchers such as Cao et al. investigated the synthesis of MXene/cellulose nanofiber composite and CNT/MXene/cellulose nanofibril composite (Cao et al., 2019). These studies explored the incorporation of MXenes as beneficial EMI-shielding nanofillers within a polymer matrix (Sun et al., 2017). The bonding of MXene materials with textiles is facilitated by their sufficient functional groups, enabling the creation of conductive fibers coated with MXene or spun from MXene, which have shown promise in the development of electrically conductive textiles (An et al., 2018; Liu et al., 2019; Uzun et al., 2019). Notably, Zhao et al. successfully deposited MXene nanosheets on cellulose fiber nonwoven fabric, resulting in MXene-based smart flexible fabric with notable Joule heating effects and rapid humidity responsiveness. Such advancements offer potential applications in personal medical therapy and mobile healthcare (Zhao et al., 2020).

In this study, we focus on the fabrication of MXene/cellulose fiber composites, utilizing a scalable and environmentally friendly dip coating technique. The dip coating process involves subjecting the composites to multiple cycles of immersion, drying, and re-immersion in an aqueous MXene solution. Through this method, we ensure a uniform and thorough coating of MXene sheets onto the surfaces of cellulose fibers, creating a well-integrated hybrid material.

To achieve optimal results, we carefully adjust the number of dip coating cycles, which allows us to control the MXene content in the composite and tailor its properties accordingly. The scalable nature of the dip coating technique makes it suitable for large-scale production and offers practical implications for potential industrial applications of these composites in various fields. Furthermore, we emphasize the eco-friendly aspect of our fabrication process, as it involves the use of readily available and sustainable cellulose fibers as the raw material. The combination of MXenes, with their exceptional electrical conductivity, and cellulose fibers, known for their flexibility and biocompatibility, holds great promise for the development of advanced materials for wearable electronic textiles, sensors, and other functional applications.

Comprehensive characterization of the resulting MXene/cellulose composites was conducted to examine their morphological and microstructural properties. Scanning electron microscopy (SEM) analysis, X-ray diffraction (XRD), and thermogravimetric analysis (TGA) were employed to investigate the structural features and thermal stability of the composites. Furthermore, the electrical characteristics and electrical heating performance of the composites were assessed. Through these analytical techniques, we aimed to elucidate the influence of different dip coating cycles on the morphology, microstructure, and electrical properties of the MXene/cellulose composites.

Experimental

Materials

Dong bang Co., Ltd. and TRUN NANO Co., Ltd. (China) provided the cellulose fiber and 0.5 wt% MXene solution, respectively. All of these chemical reagents were employed exactly as received, and deionized water was utilized during the preparation procedure.

Synthesis of MXene/cellulose fiber composites

The cellulose fiber dip coating technique began with ultrasonic treatment of the MXene solution dispersed in deionized water prior to coating, followed by coating in a continual stirring state. Figure 1 depicts a flow method for coating MXene successively on pristine cellulose fibers. The entire procedure is outlined here. A typical dip coating cycle was employed to create the MXene/cellulose fiber composites, in which the cellulose fiber was dipped in diffusion solution, stirred for 60 min, and then dried in an oven at 60 °C for 60 min. This process was simply performed four times.

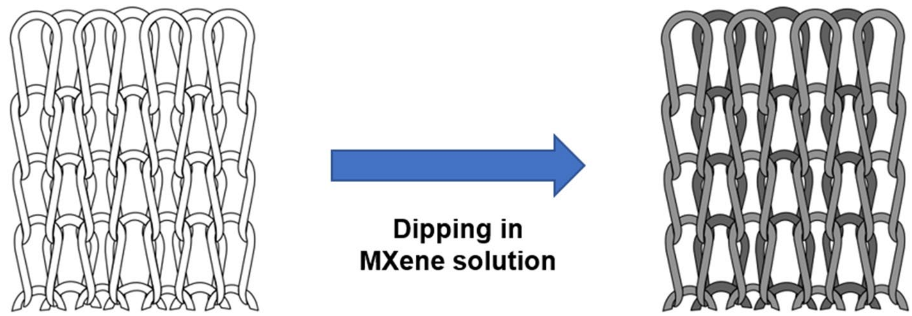

Fig. 1 Fabrication process of MXenes/cellulose hybrid fibers

Characterization

To observe the microstructure of cellulose fibers and MXene, morphological properties were investigated using a scanning electron microscope (SU8010, Hitachi) to obtain surface and cross-sectional images.

The crystalline structural features were measured by an in-situ X-ray diffractometer (Empyrean, Malvern Panel) using a 2θ angular reflection method.

The thermal property was investigated using a thermogravimetric analyzer (SETSYS Evolution, SETARAM) under Argon-gas conditions in the temperature range of 40–800 °C at a heating rate of 10 °C/min.

The electrical property was investigated by obtaining the longitudinal current–voltage (I–V) curve of the fiber using a source meter (2450 Source Meter, Keithley Instruments). For the electrical measurement, the electrode distance of the fiber was set to 10.0 mm, and the diameter that could obtain electrical conductivity was calculated using the scanning electron microscopy (SEM) images.

To test the performance of the electric heating, a voltage between 0 and 50 V is applied using the source meter. The maximal heating and average temperatures were then determined from the infrared thermal pictures that had been taken after 10 min utilizing an infrared camera (A35, FLIR systems). At room temperature and 50% relative humidity, all electric heating behavior studies have been carried out.

The mechanical properties of the knit types were characterized using a constant rate of extension type tensile-testing machine (AGS-500D, Shimadzu, Japan). The upper and lower parts of the knit were gripped at 0.5 cm. The distance between the clamps that gripped the sample was set to 2 cm. The elongation process was repeated 400 times at 50% strain.

Results and Discussion

Morphology and structure analysis

The morphology and microstructures of pure cellulose fibers and MXene/cellulose fiber composites with various coating systems and cycles may be ascertained utilizing the SEM micrographs exposed in Fig. 2. The neat cellulose fiber's smooth, spotless surface is depicted in Fig. 2a by means of a SEM image, and the cross section reveals the cotton's lumen structure. After dipping the fibers in the MXene suspension and drying, Fig. 2b–e displays the SEM images of the conductive MXene/cellulose fiber composites taken from various angles. After the flexible 2D MXene nanosheets were added, the previously

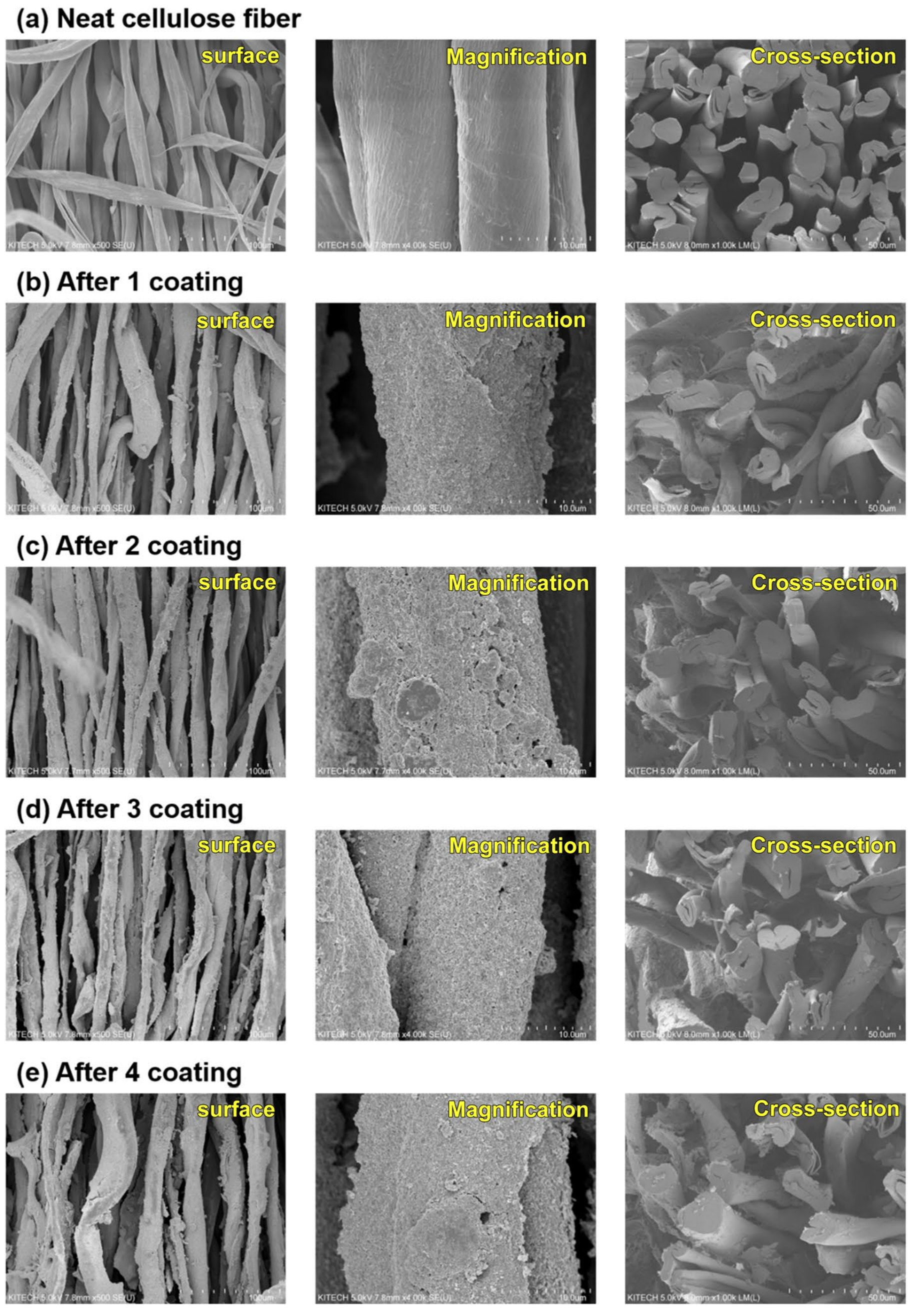

Fig. 2 SEM images of (**a**) neat cellulose fibers and (**b**–**e**) MXene/cellulose fiber composites at different surfaces, magnifications and cross sections obtained during various dip coating cycles

smooth cotton fiber surface turned rough. The assembled MXene nanosheets were then visible on the cellulose fibers. This led to the creation of cellulose fibers with MXene decorations and a core–shell structure. According to the SEM images, the dip coating cycle uniformly coats the fiber surface, with part of the coating permeating inside the fiber.

By examining X-ray diffraction patterns, this was also verified. The structural characteristics of neat cellulose fibers and MXene/cellulose hybrid fibers were examined employing the X-ray diffraction pattern shown in Fig. 3. The reflections of the (101),

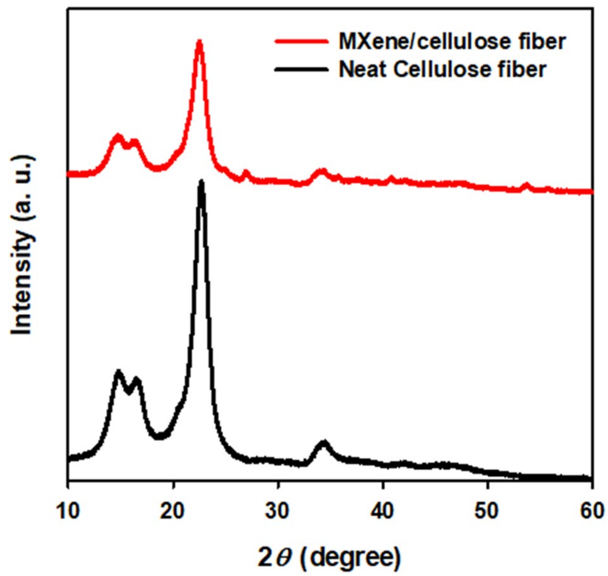

Fig. 3 X-ray diffraction pattern of neat cellulose fiber and MXene/cellulose fiber composites

(101), (002), and (040) planes of cellulose I-form crystallites with a monoclinic lattice are, respectively, connected with four intense diffraction peaks that are present in MXenes/cellulose hybrid fibers at 2θ = 14.7°, 16.3°, 22.7°, and 33.7° (Lee et al., 2016; Tang et al., 2012). The (002) crystal plane of the cellulose crystalline structure was assigned a large diffraction peak at 22.90 in Fig. 3. The strength of the (002) diffraction peak rapidly decreased as the MXene concentration increased (Lee et al., 2016). This outcome demonstrates that the dip coating method used to coat the MXene sheets on cellulose fibers is effective. In conclusion, the analytical findings offered solid proof that MXene $Ti_3C_2T_x$ nanosheets were successfully applied to the fabric surface.

Thermal gravimetric analysis

The thermogravimetric analysis (TGA) is typically carried out to further investigate thermal stability (Nie et al., 2020). Figure 4, displays the thermogravimetric (TG) and differential thermal gravity (DTG) curves. Neat cellulose fiber has two-step weight reductions, as shown in Fig. 4. After the addition of MXene nanosheets, the thermal degradation trend for cellulose fiber remains the same, despite the fact that MXene has a modest effect on T_5 and a gradual rise on T_{max}. The excellent thermal conductivity of MXene, which serves as a heat source to cause the disintegration of cellulose fiber at a lower temperature, is primarily blamed for the decrease in thermal stability. This will surely have an impact on the electrical properties and strain sensing capabilities of MXene/cellulose hybrid fiber composites at higher working temperatures. However, the MXene/cellulose hybrid fiber composite still has significant potential to operate over a wider temperature range than other conventional polymer-based strain sensors because of the exceptional thermal stability of the cellulose fibers. At temperatures greater than 400 °C, both samples entirely evaporated. But as can be seen from the DTG curves (Fig. 4), the maximal weight loss rate of the MXenes/cellulose hybrid fiber composite is significantly lower

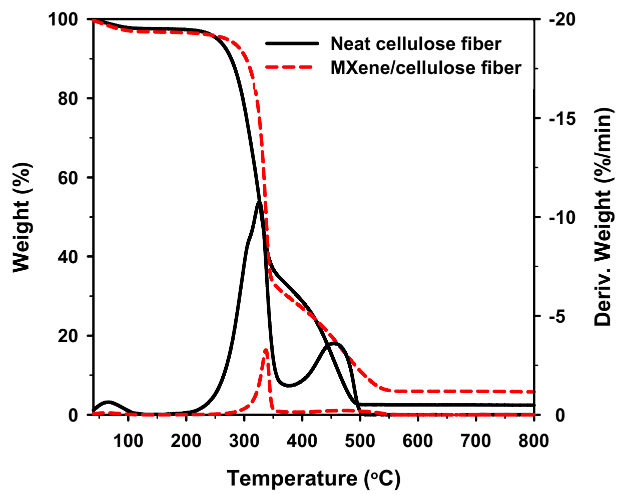

Fig. 4 Neat cellulose fiber and MXene/cellulose fiber composites TG and DTG curves

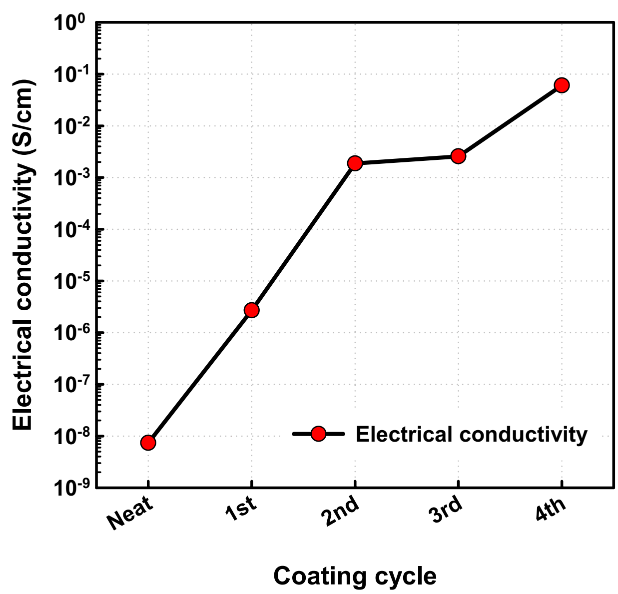

Fig. 5 Electrical properties of neat cellulose fiber and MXene/cellulose fiber composites on the longitudinal direction

than that of cellulose fiber. It might be because MXene's "barrier effect" prevents the diffusion of volatile chemicals and the passage of heat.

Electrical conductivity

Figure 5 illustrates the electrically conductive properties of neat cellulose fiber and MXene at various coating cycles. The electrical conductivity of $Ti_3C_2T_x$/cellulose fiber composites exhibits a clear enhancement as the $Ti_3C_2T_x$ coating increases. It is evident that the electrical conductivity of the $Ti_3C_2T_x$/cellulose fiber composite significantly rises with the addition of the $Ti_3C_2T_x$ coating. The conductivity of the $Ti_3C_2T_x$/cellulose fiber composites notably increases when the $Ti_3C_2T_x$ coating is increased to 4, indicating the formation of a conductive $Ti_3C_2T_x$ network within the cellulose fiber matrix. The composite fibers' conductivity gradually improves with an increase in $Ti_3C_2T_x$ concentration, owing to the establishment of a reliable conductive pathway. The addition of MXene does not cause abrupt changes in electrical conductivity, and the alteration in electrical conductivity generally exhibits a consistent pattern of change when the concentration of MXene coating is adjusted at higher levels (4 coatings). The electrical conductivity of neat cellulose fiber is measured as 7.38×10^{-9} at the non-conductive level, which eventually increases to 0.06 S/cm upon completion of the fourth coating. We specifically examine the conductivity of 1 to 4 coatings in this experiment, as the transition in electrical conductivity becomes more gradual after the fourth MXene coating.

The current–voltage (I–V) and electric power-voltage (P–V) graphs of the MXene/cellulose hybrid fibers produced by the dip coating cycle technique are presented in Fig. 6. Voltage-dependent electric current and power variations in thickness and in plane directions of the MXene/cellulose hybrid fiber composite made with various dip coating sequences and cycles have been reached to explore the electric properties of the hybrid cellulose fibers. In the current–voltage (I–V) plots in the plane direction, the neat cellulose fibers exhibit no electric current variation over the applied voltage range of up to 40 V (Fig. 6a). For all hybrid cellulose fibers, the electric current rises linearly with applied voltage, with the slope of the I-V plots being steeper for fibers with higher dip coating cycles. The hybrid cellulose fibers with the MXene top-coating layer display greater slopes of I-V plots, when the number of dip coating cycles is the same. According to the above apparent thickness, it reveals that MXene layers are alternately coated on the cellulose fibers over the constant dip coating cycle. Figure 6b depicts both the calculation and graphical representation of the $P = IV$ equation based on the I–V plots. We can demonstrate that electrical power increases in direct proportion to the applied voltage in each sample.

Electric heating behavior

The MXene/cellulose hybrid fiber composite material's high electrical conductivity and flexibility make wearable heaters for personal thermal management systems possible. Heat can be produced by collisions between accelerated electrons and phonons in conductive fabrics when a current flow through them. Some of the reported

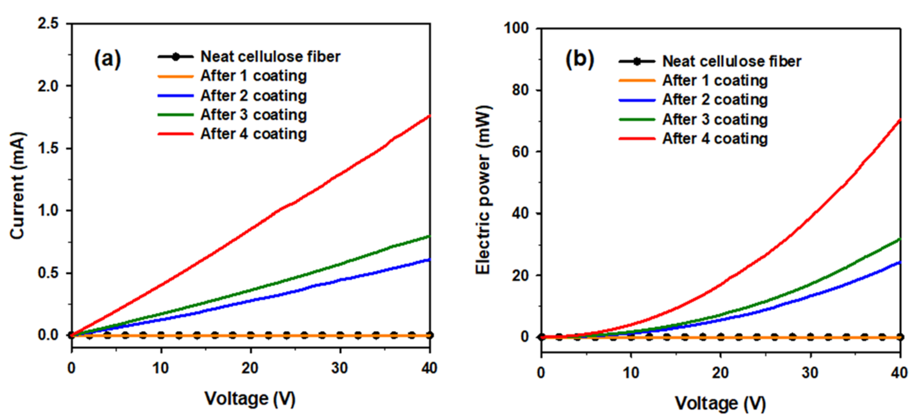

Fig. 6 The hybrid cellulose fiber of (**a**) current–voltage (I–V) and (**b**)electric power-voltage (P–V) plots.

conductive materials for Joule heating elements at the time were AgNWs, CuNWs, PEDOT, GO, and CNTs (Guo et al., 2017; Hazarika et al., 2018; Zhang et al., 2017). A 2 cm length of MXene/cellulose fiber composite was cut, and both ends were held with forceps as electrodes at 0.5 cm intervals. Subsequently, only a 1 cm section, representing the actual heating area, was connected to a DC power source, and the surface temperature distribution was recorded using an infrared camera, as depicted in Fig. 7. The inset image in Fig. 7 clearly illustrates the red glow emitted by the heating area compared to the ambient temperature, validating the experimental procedure. Voltages ranging from 10 to 50 V were applied, and it was observed that the heating temperature increased linearly, except when the overvoltage reached 50 V. Additionally, in accordance with the National Agency for Technology and Standards' announcement of KC 60335-2-17, which pertains to the 'Technical Standards for Telecommunication Products and Parts,' the conductor-fabric heater is permitted to exceed 50 °C for a maximum duration of 2 h, but it must not surpass 85 °C. As outlined in KC 10018, if the surface material of heated mats and beds is textile, the surface temperature should not exceed 70 °C. Notably, prolonged skin exposure to temperatures of 45 °C can result in second and third-degree burns (Choi et al., 2023; Shuvo et al., 2021). Based on this electric heating behavior, these results can be used as basic data when manufacturing an actual heater with a larger area.

These results demonstrate the excellent conductivity of the developed MXene/cellulose fiber composites, opening up exciting possibilities for applications. These composites provide a solid foundation for a variety of electronic devices, including cellulosecellulose-based electrical devices (Pal et al., 2017). Due to their inherent flexibility, cost-effective production, and user-friendly design, they hold significant potential in various industries, especially in the fast-growing EE-textile sector. They can be utilized in a variety of applications, such as designing medical heating patches.

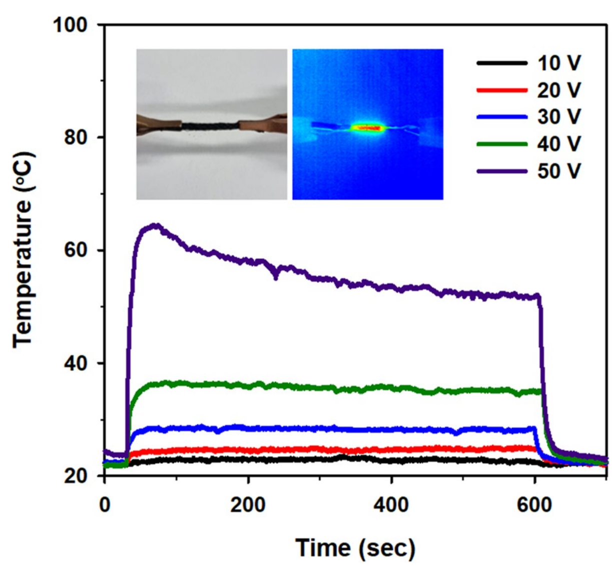

Fig. 7 Electrothermal infrared images and time-dependent temperature changes of under different applied voltages

Long term recycling behavior

The long-term recycling performance of an electric-heating factor must be carefully considered while determining its stability (Li et al., 2020). Figure 8a shows that during repeated elongation, a load of 7.8 N at a strain of up to 50% can be determined in the range of 4–7.8 N. Based on the structural features of the knit, this result is mostly generated by deformation of the knit structure rather than a linear drop. As a result of repeated stretching, slight structural deformations may happen, but the fibers are not split or harmed. Figure 8b, illustrates the repeated elongation result, which calculates the knit's resistance based on 400 cycles. In comparison to the initial resistance, the resistance rises from 51 kΩ to 250 kΩ after 400 cycles. Nevertheless, the resistance decreases to around 86 kΩ when one coat of MXene is added after 400 cycles. Given the simplicity of the coating process, our findings indicate that incorporating just one additional coating enables ample reusability, even under the influence of mechanical forces exerted on the knit material. On the other side, there have been various reports on electrically conductive properties (Cao et al., 2018; Feng et al., 2022; Liu et al., 2022; Zhan et al., 2019; Zhou et al., 2021). Our study used a very small amount of MXene at a concentration of 0.5 wt% compared to other studies, and given the simplicity of the coating procedure, the result is that the coating is applied once more to the nits to protect them from the applied physical forces. This demonstrates that sufficient reuse can be achieved.

Conclusions

In conclusion, extremely flexible MXene/cellulose fiber composites were effectively produced utilizing a simple dip-coating method. As observed in the SEM micrographs of the cellulose hybrid fiber's surface and cross section, MXene is successively coated while remaining somewhat present in the internal of the fiber. The loss in thermal stability is mostly attributed to MXene's superior thermal conductivity, which acts as a heat source to trigger the breakdown of cellulose fiber at a lower temperature. The electrical characteristics and strain sensing capabilities of the MXenes/cellulose fiber composite at higher operating temperatures will undoubtedly be impacted by this. The electrical conductivity of the cellulose fibers supports this coating process. In the in-plane current–voltage (*I–V*) plots, no current change was observed for the pure cellulose fibers over the applied voltage range up to 40 V. The slope of the *I–V* plots is greater for the MXene/

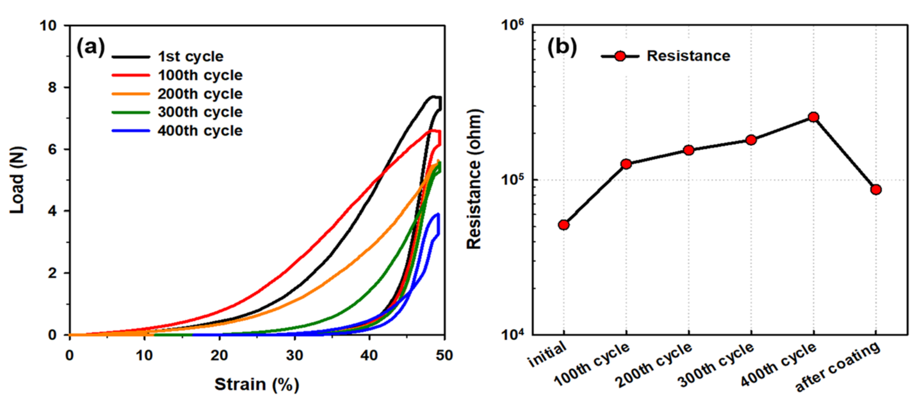

Fig. 8 Measuring variations in rib-stitched knit recycling efficiency (**a**) Tensile strength (**b**) Resistance after 400 times of elongations at 50% strain

cellulose hybrid fiber with more dip coating cycles, and the electric current increases linearly with applied voltage for all hybrid cellulose fibers. Additionally, the thermally stable MXene/cellulose hybrid fibers' electrical-heating capability has been validated up to 250 °C. Because of its great flexibility and other applications needing electrical heating, the cellulose/MXene hybrid fiber as a whole has shown potential for employment in the E-textile business. It was produced using an effective dip coating procedure.

Furthermore, our hybrid conductive material presents significant potential for the development of cellulose-based electrical devices. These devices, featuring electric heating capabilities, can find versatile applications such as heated clothing, garments with temperature regulation, and medical heating patches (Wang et al., 2016). Additionally, cellulose-based electrical devices hold great promise in the sensing and smart-clothing field. With ongoing research and development, we expect continuous improvements in the performance and functionality of these cellulose-based electrical devices, harnessing the distinctive properties of our MXene/cellulose fiber composite.

Authors' contributions
H.Y.C. conceived the research topic. Y.H.C. performed all experiments. J.K.K. and H.J.C assisted in the interpretation of the results. C.P. helped with proofreading the English text and organizing the paper. C.S.L. is largely responsible for electrical heating. All authors discussed and reviewed the manuscript and agreed to its submission.

Funding
1. Following are the results of a study on the "Leaders in Industry-University Cooperation 3.0" Project, supported by the Ministry of Education and the National Research Foundation of Korea. 2. This research was supported by the Government-wide R&D Fund for Infections Disease Research (GFID), funded by the Ministry of the Interior and Safety, Republic of Korea (Grant number: 20016180).

Availability of data and materials
The datasets used and/or analyzed during the current study are available from the corresponding author on reasonable request.

Declarations

Competing interests
The authors declare that they have no competing interests

Received: 13 June 2023 Accepted: 2 August 2023
Published online: 02 January 2024

References
Alhabeb, M., Maleski, K., Anasori, B., Lelyukh, P., Clark, L., Sin, S., & Gogotsi, Y. (2017). Guidelines for synthesis and processing of two-dimensional titanium carbide ($Ti_3C_2T_x$ MXene). *Chemistry of Materials, 29*, 7633–7644. https://doi.org/10.1021/acs.chemmater.7b02847.

An, H., Habib, T., Shah, S., Gao, H., Radovic, M., Green, M. J., & Lutkenhaus, J. L. (2018). Surface-agnostic highly stretchable and bendable conductive MXene multilayers. *Science Advances, 4*, Article eaaq0118. https://doi.org/10.1126/sciadv.aaq0118.

Cao, M.-S., Cai, Y.-Z., He, P., Shu, J.-C., Cao, W.-Q., & Yuan, J. (2019). 2D MXenes: Electromagnetic property for microwave absorption and electromagnetic interference shielding. *Chemical Engineering Journal, 359*, 1265–1302. https://doi.org/10.1016/j.cej.2018.11.051.

Cao, W. T., Chen, F. F., Zhu, Y. J., Zhang, Y. G., Jiang, Y. Y., Ma, M. G., & Chen, F. (2018). Binary strengthening and toughening of MXene/cellulose nanofiber composite paper with nacre-inspired structure and superior electromagnetic interference shielding properties. *ACS Nano, 12*, 4583–4593. https://doi.org/10.1021/acsnano.8b00997.

Chen, G., Li, Y., Bick, M., & Chen, J. (2020). Smart textiles for electricity generation. *Chemical Reviews, 120*(8), 3668–3720. https://doi.org/10.1021/acs.chemrev.9b00821.

Chen, Z., Hu, Y., Zhuo, H., Liu, L., Jing, S., Zhong, L., Peng, X., & Sun, R. (2019). Compressible, elastic, and pressure-sensitive carbon aerogels derived from 2D titanium carbide nanosheets and bacterial cellulose for wearable sensors. *Chemistry of Materials, 31*, 3301–3312. https://doi.org/10.1021/acs.chemmater.9b00259.

Choi, H. Y. (2023). Study on the microstructure, electrical properties, and electric-heating performance of MWCNT/AgNW/cellulose hybrid fibers. *The Journal of the Textile Institute, 114*(4), 613–621. https://doi.org/10.1080/00405000.2022.2057639.

Cui, C., Xiang, C., Geng, L., Lai, X., Guo, R., Zhang, Y., Xiao, H., Lan, J., Lin, S., & Jiang, S. (2019). Flexible and ultrathin electrospun regenerate cellulose nanofibers and d-$Ti_3C_2T_x$ (MXene) composite film for electromagnetic interference shielding. *Journal of Alloys and Compounds, 788*, 1246–1255. https://doi.org/10.1016/j.jallcom.2019.02.294.

Feng, S., Yi, Y., Chen, B., Deng, P., Zhou, Z., & Lu, C. (2022). Rheology-guided assembly of a highly aligned MXene/Cellulose nanofiber composite film for high performance electromagnetic interference shielding and infrared stealth. *ACS Applied Materials and Interfaces, 14*, 36060–36070. https://doi.org/10.1021/acsami.2c11292.

Gao, W., Ota, H., Kiriya, D., Takei, K., & Javey, A. (2019). Flexible electronics toward wearable sensing. *Accounts of Chemical Research, 52*(3), 523–533. https://doi.org/10.1021/acs.accounts.8b00500

Guo, Y., Dun, C. C., Xu, J. W., Mu, J. K., Li, P. Y., Gu, L. W., Hou, C. Y., Hewitt, C. A., Zhang, Q. H., Li, Y. G., Carroll, D. L., & Wang, H. Z. (2017). Ultrathin, washable, and large-area graphene papers for personal thermal management. *Small*, *13*(44), Article e1702645. https://doi.org/10.1002/smll.201702645.

Hazarika, A., Deka, B. K., Kim, D., Jeong, H. E., Park, Y. B., & Park, H. W. (2018). Woven Kevlar fiber/polydimethylsiloxane/reduced graphene oxide composite-based personal thermal management with freestanding Cu-Ni core-shell nanowires. *Nano Letters, 18*, 6731–6739. https://doi.org/10.1021/acs.nanolett.8b02408.

Kim, H., & Lee, S. (2018). Characterization of carbon nanofiber (CNF)/polymer composite coated on cotton fabrics prepared with various circuit patterns. *Fashion and Textiles, 5*, Article 7. https://doi.org/10.1186/s40691-017-0120-2.

Kim, H., & Lee, S. (2020). Characterization of electrical heating of graphene/PLA honeycomb structure composite manufactured by CFDM 3D printer. *Fashion and Textiles, 7*, Article 8. https://doi.org/10.1186/s40691-020-0204-2.

Kim, S. J., Kim, S. U., Vu, C. C., & Kim, J. Y. (2023). Improved heating method for shape-memory alloy using carbon nanotube and silver paste. *Fashion and Textiles, 10*(1), Article 16. https://doi.org/10.1186/s40691-023-00331-1.

Lee, T.-W., Lee, S.-E., & Jeong, Y. G. (2016). Highly effective electromagnetic interference shielding materials based on silver nanowire/cellulose papers. *ACS Applied Materials and Interfaces, 8*, Article 13123. https://doi.org/10.1021/acsami.6b02218.

Lee, Y., Park, J., Choe, A., Cho, S., Kim, J., & Ko, H. (2020). Mimicking human and biological skins for multifunctional skin electronics. *Advanced Functional Materials, 30*, Article 1904523. https://doi.org/10.1002/adfm.201904523.

Lei, Z., Wang, Q., Sun, S., Zhu, W., & Wu, P. (2017). A bioinspired mineral hydrogel as a selfhealable, mechanically adaptable ionic skin for highly sensitive pressure sensing. *Advanced Materials, 29*, Article 1700321. https://doi.org/10.1002/adma.201700321.

Li, X., Koh, K. H., Farhan, M., & Lai, K. W. C. (2020). An ultra-flexible polyurethane yarn-based wearable strain sensor with a polydimethylsiloxane infiltrated multilayer sheath for smart textiles. *Nanoscale, 12*(6), 4110–4118. https://doi.org/10.1039/C9NR09306K.

Liang, L., Han, G., Li, Y., Zhao, B., Zhou, B., Feng, Y., Ma, J., Wang, Y., Zhang, R., & Liu, C. (2019). Promising $Ti_3C_2T_x$ MXene/Ni chain hybrid with excellent electromagnetic wave absorption and shielding capacity. *ACS Applied Materials and Interfaces, 11*, 25399–25409. https://doi.org/10.1021/acsami.9b07294.

Liu, D., Gao, Y., Song, Y., Zhu, H., Zhang, L., Xie, Y., Shi, H., Shi, Z., Yang, Q., & Xiong, C. (2022). Highly sensitive multifunctional electronic skin based on nanocellulose/MXene composite films with good electromagnetic shielding biocompatible antibacterial properties. *Biomacromolecules, 23*, 182–195. https://doi.org/10.1021/acs.biomac.1c01203.

Liu, J., Zhang, H. B., Sun, R., Liu, Y., Liu, Z., Zhou, A., & Yu, Z. Z. (2017). Hydrophobic, flexible, and lightweight MXene foams for high-performance electromagnetic-interference shielding. *Advanced Materials, 29*, Article 1702367. https://doi.org/10.1002/adma.201702367.

Liu, L. X., Chen, W., Zhang, H. B., Wang, Q. W., Guan, F. L., & Yu, Z. Z. (2019). Flexible and multifunctional silk textiles with biomimetic leaf-like MXene/Silver nanowire nanostructures for electromagnetic interference shielding, humidity monitoring, and self-derived hydrophobicity. *Advanced Functional Materials, 29*, Article 1905197. https://doi.org/10.1002/adfm.201905197.

Liu, Y., Zheng, H., Zhao, L., Liu, S., Yao, K., Li, D., Yiu, C., Gao, S., Avila, R., Pakpong, C., Chang, L., Wang, Z., Huang, X., Xie, Z., Yang, Z., & Yu, X. (2020). Electronic skin from high throughput fabrication of intrinsically stretchable lead zirconate titanate elastomer. *Research, 2020*, Article 1085417. https://doi.org/10.34133/2020/1085417.

Naguib, M., Mochalin, V. N., Barsoum, M. W., & Gogotsi, Y. (2014). 25th Anniversary Article: MXenes: A new family of two-dimensional materials. *Advanced Materials, 26*, 992–1005. https://doi.org/10.1002/adma.201304138.

Nie, S., Jin, D., Xu, Y., Han, C., Dong, X., & Yang, J.-N. (2020). Effect of a flower-like nickel phyllosilicate-containing iron on the thermal stability and flame retardancy of epoxy resin. *Journal of Materials Research and Technology, 9*, 10189–10197. https://doi.org/10.1016/j.jmrt.2020.07.021.

Pal, A., Cuellar, H. E., Kuang, R., Caurin, H. F., Goswami, D., & Martinez, R. V. (2017). Self-powered, paper-based electrochemical devices for sensitive point-of-care testing. *Advanced Materials Technologies, 2*, Article 1700130. https://doi.org/10.1002/admt.201700130.

Seyedin, S., Zhang, P., Naebe, M., Qin, S., Chen, J., Wang, X., & Razal, J. M. (2019). Textile strain sensors: A review of the fabrication technologies, performance evaluation and applications. *Materials Horizons, 6*, 219–249. https://doi.org/10.1039/C8MH01062E.

Shahzad, F., Alhabeb, M., Hatter, C. B., Anasori, B., Hong, S. M., Koo, C. M., & Gogotsi, Y. (2016). Electromagnetic interference shielding with 2D transition metal carbides (MXenes). *Science, 353* (6304), 1137–1140. https://doi.org/10.1126/science.aag2421.

Shuvo, I. I., Decaens, J., Lachapelle, D., & Dolez, P. I. (2021). Smart textiles testing: A road map to standardized test methods for safety and quality-control. *Textiles for Advanced Applications*. https://doi.org/10.5772/intechopen.96500.

Sun, R., Zhang, H. B., Liu, J., Xie, X., Yang, R., Li, Y., Hong, S., & Yu, Z. Z. (2017). Highly conductive transition metal carbide/carbonitride (MXene)@polystyrene nanocomposites fabricated by electrostatic assembly for highly efficient electromagnetic interference shielding. *Advanced Functional Materials, 27*, Article 1702807. https://doi.org/10.1002/adfm.201702807.

Tang, S., Baker, G. A., Ravula, S., Jones, J. E., & Zhao, H. (2012). PEG-functionalized ionic liquids for cellulose dissolution and saccharification. *Green Chemistry, 14*(10), 2922–2932. https://doi.org/10.1039/C2GC35631G.

Trung, T. Q., & Lee, N. E. (2016). Flexible and stretchable physical sensor integrated platforms for wearable human-activity monitoring and personal healthcare. *Advanced Materials, 28*(22), 4338–4372. https://doi.org/10.1002/adma.201504244.

Uzun, S., Seyedin, S., Stoltzfus, A. L., Levitt, A. S., Alhabeb, M., Anayee, M., Strobel, C. J., Razal, J. M., Dion, G., & Gogotsi, Y. (2019). Knittable and washable multifunctional MXene-coated cellulose yarns. *Advanced Functional Materials, 29*, Article 1905015. https://doi.org/10.1002/adfm.201905015.

Wang, C., Xia, K., Wang, H., Liang, X., Yin, Z., & Zhang, Y. (2019a). Advanced carbon for flexible and wearable electronics. *Advanced Materials, 31*(9), 1801072. https://doi.org/10.1002/adma.201801072.

Wang, C.-C., Hennek, J. W., Ainla, A., Kumar, A. A., Lan, W.-J., Im, J., Smith, B. S., Zhao, M., & Whitesides, G. M. (2016). A paper-based "pop-up" electrochemical device for analysis of beta-hydroxybutyrate. *Analytical Chemistry, 88*, 6326–6333. https://doi.org/10.1021/acs.analchem.6b00568.

Wang, L., Liu, W., Yan, Z., Wang, F., & Wang, X. (2020). Stretchable and shape-adaptable triboelectric nanogenerator based on biocompatible liquid electrolyte for biomechanical energy harvesting and wearable human–machine interaction. *Advanced Functional Materials, 31*, Article 2007221. https://doi.org/10.1002/adfm.202007221.

Wang, Q. W., Zhang, H. B., Liu, J., Zhao, S., Xie, X., Liu, L., Yang, R., Koratkar, N., & Yu, Z. Z. (2019b). Multifunctional and water-resistant MXene-decorated polyester textiles with outstanding electromagnetic interference shielding and joule heating performances. *Advanced Functional Materials, 29*, Article 1806819. https://doi.org/10.1002/adfm.201806819.

Wu, N., Cheng, X., Zhong, Q., Zhong, J., Li, W., Wang, B., Hu, B., & Zhou, J. (2015). Cellular polypropylene piezoelectric for human body energy harvesting and health monitoring. *Advanced Functional Materials, 25*(30), 4788–4794. https://doi.org/10.1002/adfm.201501695.

Yang, J., Mun, J., Kwon, S. Y., Park, S., Bao, Z., & Park, S. (2019). Electronic skin: Recent progress and future prospects for skin-attachable devices for health monitoring, robotics, and prosthetics. *Advanced Materials, 31*, Article 1904765. https://doi.org/10.1002/adma.201904765.

Yin, R., Yang, S., Li, Q., Zhang, S., Liu, H., Han, J., Liu, C., & Shen, C. (2020). Flexible conductive Ag nanowire/cellulose nanofibril hybrid nanopaper for strain and temperature sensing applications. *Science Bulletin, 65*, 899–908. https://doi.org/10.1016/j.scib.2020.02.020.

Yue, Y., Liu, N., Liu, W., Li, M., Ma, Y., Luo, C., Wang, S., Rao, J., Hu, X., Su, J., Zhang, Z., Huang, Q., & Gao, Y. (2018). 3D hybrid porous Mxene-sponge network and its application in piezoresistive sensor. *Nano Energy, 50*, 79–87. https://doi.org/10.1016/j.nanoen.2018.05.020.

Zhan, Z., Song, Q., Zhou, Z., & Lu, C. (2019). Ultrastrong and conductive MXene/cellulose nanofiber films enhanced by hierarchical nano-architecture and interfacial interaction for flexible electromagnetic interference shielding. *J. Mater. Chem. C, 7*, 9820–9829. https://doi.org/10.1039/C9TC03309B.

Zhang, M., Zhao, M., Jian, M., Wang, C., Yu, A., Yin, Z., Liang, X., Wang, H., Xia, K., Liang, X., Zhai, J., & Zhang, Y. (2019). Printable smart pattern for multifunctional energy management e-textile. *Matter, 1*(1), 168–179. https://doi.org/10.1016/j.matt.2019.02.003.

Zhang, M. C., Wang, C. Y., Liang, X. P., Yin, Z., Xia, K. L., Wang, H., Jian, M. Q., & Zhang, Y. Y. (2017). Weft-knitted fabric for a highly stretchable and low-voltage wearable heater. *Adv. Electron. Mater, 3*(9), Article 1700193. https://doi.org/10.1002/aelm.201700193.

Zhang, Y., He, P., Luo, M., Xu, X., Dai, G., & Yang, J. (2020). Highly stretchable polymer/silver nanowires composite sensor for human health monitoring. *Nano Research, 13*(4), 919–926. https://doi.org/10.1007/s12274-020-2730-z.

Zhao, X., Wang, L.-Y., Tang, C.-Y., Zha, X.-J., Liu, Y., Su, B.-H., Ke, K., Bao, R.-Y., Yang, M.-B., & Yang, W. (2020). Smart $Ti_3C_2T_x$ MXene fabric with fast humidity response and joule heating for healthcare and medical therapy applications. *ACS Nano, 14*, 8793. https://doi.org/10.1021/acsnano.0c03391.

Zhong, J., Ma, Y., Song, Y., Zhong, Q., Chu, Y., Karakurt, I., Bogy, D. B., & Lin, L. (2019). A flexible piezoelectret actuator/sensor patch for mechanical human-machine interfaces. *ACS Nano, 13*(6), 7107–7116. https://doi.org/10.1021/acsnano.9b02437.

Zhou, B., Li, Q., Xu, P., Feng, Y., Ma, J., Liu, C., & Shen, C. (2021). An asymmetric sandwich structural cellulose-based film with self-supported MXene and AgNW layers for flexible electromagnetic interference shielding and thermal management. *Nanoscale, 13*, 2378–2388. https://doi.org/10.1039/D0NR07840A.

Zhou, B., Zhang, Z., Li, Y., Han, G., Feng, Y., Wang, B., Zhang, D., Ma, J., & Liu, C. (2020). Flexible, robust, and multifunctional electromagnetic interference shielding film with alternating cellulose nanofiber and MXene layers. *ACS Applied Materials and Interfaces, 12*, 4895–4905. https://doi.org/10.1021/acsami.9b19768.

Publisher's Note

Chan Sol Kang is a associate professor in Shinhan University.

Jong Kyu Kim is a professor in Shinhan University.

Chae-Seok Lee is a researcher (Ph.D.) in KAIST Institute for Information Technology Convergence Intergrated Sensor Team, KAIST.

HoJong Chang is a professor in KAIST Institute for Information Technology Convergence Intergrated Sensor Team, KAIST.

Yeong Heon Cho is a researcher (undergraduate) KAIST Institute for Information Technology Convergence Intergrated Sensor Team, KAIST.

Cheera Prasad is a researcher (Ph.D.) in Dong-A University.

Hyeong Yeol Choi is a assistant professor in Dong-A University.